coatings

MDPI

Article

Fabrication and Sterilization Characteristics of Visible Light Photocatalyst of CuO/ZrO_2/CB/Coal-Tar-Pitch-SAC

Ziang Xu [1], Guiying Xu [1,*], Beibei Han [2], Kun Wang [1,*], Hui Ge [3], Baigang An [1], Dongying Ju [2], Maorong Chai [2], Lixiang Li [1] and Weimin Zhou [1,*]

[1] Key Laboratory of Energy Materials and Electrochemistry Research Liaoning Province, University of Science and Technology Liaoning, Anshan 114051, China; ziangxu6564@163.com (Z.X.); baigang73@126.com (B.A.); lxli2005@126.com (L.L.)

[2] Advanced Science Research Laboratory, Saitama Institute of Technology, Fusaiji 1690, Japan; hanbeibei@nimte.ac.cn (B.H.); dyju@sit.ac.jp (D.J.); chaimaorong@spic.com.cn (M.C.)

[3] Qidian Photocatlyst Co., Ltd., Anshan 114051, China; gehui7777@126.com

* Correspondence: xuguiying751107@ustl.edu.cn (G.X.); wk172860@ustl.edu.cn (K.W.); aszhou@ustl.edu.cn (W.Z.)

Abstract: To provide an effective method of green aquaculture, the photocatalysts of CuO/ZrO_2/CB/coal-tar-pitch-SAC, which have visible light sterilization capacity, were successfully fabricated by coating ZrO_2 and CuO on the surface of CB/coal-tar-pitch-SAC. The structures of synthesized CuO/ZrO_2/CB/coal-tar-pitch-SAC were investigated by XRD, XPS and SEM measurements in detail. It was observed that CuO/ZrO_2/CB/coal-tar-pitch-SAC materials possess obvious heterojunction structure and excellent visible light sterilization capacity when the prepared weight ratio of CuO, ZrO_2 and CB/coal-tar-pitch-SAC is controlled as 0.03:0.3:1. Our studies can provide a beneficial reference for the design of photocatalysts with sterilization capacity in visible light.

Keywords: photocatalyst; heterojunction; coal tar pitch; green aquaculture; ZrO_2

Citation: Xu, Z.; Xu, G.; Han, B.; Wang, K.; Ge, H.; An, B.; Ju, D.; Chai, M.; Li, L.; Zhou, W. Fabrication and Sterilization Characteristics of Visible Light Photocatalyst of CuO/ZrO_2/CB/Coal-Tar-Pitch-SAC. *Coatings* **2021**, *11*, 816. https://doi.org/10.3390/coatings11070816

Academic Editor: Alexandru Enesca

Received: 1 June 2021
Accepted: 1 July 2021
Published: 6 July 2021

1. Introduction

Overuse of antibiotic and chemical reagents is becoming a popular aquaculture practice in China. This process severely worsens water quality and threatens the safety of food. Additionally, long-term usage of antibiotic and chemical reagents also causes the harmful bacteria to produce strong resistance to drugs. Oxidant reagents and electrolysis methods are also widely utilized in treating aquaculture [1–5]. Although these methods are capable of sterilization, the water quality is damaged. Therefore, how to develop environmentally friendly sterilizing reagents to achieve green aquaculture is becoming a pivotal issue that urgently needs to be solved. Photocatalysts are of particular interest because they exhibit excellent sterilization ability and environmentally friendly characteristics. In particular, TiO_2 as a photocatalyst has attracted much attention since it was reported by Fujishima et al. [6,7].

It is well-known that coating catalysts on the surface of active carbon (AC) is an effective way to enhance the catalyst activity [8,9]. Recently, our research group explored TiO_2 and coal-tar-pitch based spherical activated carbon containing carbon black (CB/coal-tar-pitch-SAC) and successfully prepared the novel photocatalyst of TiO_2/CB/coal-tar-pitch-SAC [10]. Strong sterilization characteristics of TiO_2/CB/coal-tar-pitch-SAC were observed and described in detail. Interestingly, TiO_2/CB/coal-tar-pitch-SAC also possesses sterilization capacity under irradiation of visible light. Our studies further indicated that CB/coal-tar-pitch-SAC as a photocatalyst support can enhance the activities of photocatalysts due to its large surface area, excellent conductivity, good fluidity and other traits.

On the other hand, it is acknowledged that the ZrO_2 compound possesses high wear resistance [11]. Thus, in order to increase the durability of the photocatalyst in actual sterilization cases, ZrO_2 as a photocatalyst should be considered preferentially.

Nevertheless, the fact that ZrO_2 compound possesses a broad valance band (5.0 eV) makes excitation by visible light difficult [11–14].

In general, fabricating the heterojunction among different semi-conductors is an effective way to improve the photosensitivity of metal oxides such as ZrO_2, TiO_2, ZnO and so on [15–20]. CuO is extensively used to fabricate photocatalysts with complex type because it possesses a narrow valance band (1.4 eV) [21]. As an example, Zhu et al. deposited CuO nanoparticles on the surface of ZnO so as to fabricate CuO/ZnO composite materials with 0D/3D structures. The fabricated materials possess excellent photodegradation for phenol with a degradation rate of 78.0% [22]. Additionally, CeO_2/CuO composite materials were fabricated with a facile co-precipitation method, and their high photodegradation for methylene blue (degradation rate of 85.7%) was observed and reported [23].

Thus, on the basis of aforementioned descriptions, in this presented study, we also attempted to use the formation of a heterojunction among both metal oxides of CuO and ZnO_2 to improve the photosensitivity of ZrO_2. Referring to our presented studies on fabrication of TiO_2/CB/coal-tar-pitch-SAC, we firstly and successfully prepared the novel CuO/ZrO_2/CB/coal-tar-pitch-SAC photocatalyst by using the same CB/coal-tar-pitch-SAC as a photocatalyst support. As a result, it was verified that CuO/ZrO_2/CB/coal-tar-pitch-SAC manifested a remarkable sterilization effect under irradiation of visible light compared with ZrO_2/CB/coal-tar-pitch-SAC, which did not show an obvious sterilization capacity in the same lighting conditions.

2. Materials and Methods

2.1. Materials

Coal tar pitch was obtained from Ansteel Group Corporation (Anshan, China). Polyvinyl alcohol (PVA) was purchased from Aladdin Industrial Corporation (Shanghai, China). $Cu(NO_3)_2 \cdot 3H_2O$ (CAS Number C140879) and $ZrOCl_2 \cdot 8H_2O$ (CAS Number Z104931) compounds were purchased from Shanghai Aladdin Biochemical Technology Co., Ltd. (Shanghai, China) Nutrient agar was purchased from Hangzhou Baisi biotech Co., Ltd. (Hangzhou, China).

2.2. Characterization

The measurements of X-ray diffraction (XRD) used the X'pert Powder instrument from PANalytical, The Netherlands. The X-ray photoelectron spectroscopy (XPS) measurements were carried out using a K-Alpha instrument from Thermo Fisher Scientific, Waltham, MA, USA. Xenon lamp (CEL-HXF300-T3) was purchased from Beijing Zhong Jiao Jin Yuan Co., Ltd. (Beijing, China). Nitrogen adsorption and desorption isotherms were measured with a Quadrasorb autosorb-iQ surface analyzer, which was purchased from Quantachrome Instruments, Boynton Beach, FL, USA [24]. Specific surface areas were determined in detail, according to the Brunauer–Emmett–Teller (BET) method. The pore size distribution was assessed with the DFT model for slit pores [25,26]. Scanning electron microscope (SEM) morphologies were evaluated with a microscope from Carl Zeiss AG, Jena, Germany. A high-pressure steam sterilizer (LDZX-50KBS) made by Shanghai Shenan medical instrument factory (Shanghai, China) was also used. An electro-heating standing-temperature cultivator was purchased from Shanghai Jinghong Laboratory Co., Ltd. (Shanghai, China).

2.3. Preparation of ZrO_2/CB/Coal-Tar-Pitch-SAC

In accordance with our previous studies, the CB/coal-tar-pitch-SAC was prepared firstly [10]. Thereafter, $ZrOCl_2 \cdot 8H_2O$ (3 g) and anhydrous alcohol (30 mL) were added to a beaker. After the obtained mixture had been stirred for 20 min at room temperature, the deionized water (30 mL) was added. The obtained mixture was stirred until the $ZrOCl_2 \cdot 8H_2O$ dissolved completely. Furthermore, the temperature of the obtained mixture was increased to 70 °C, and this mixture was stirred for 40 min.

The CB/coal-tar-pitch-SAC (1.0 g) and mixture precursor solution containing $ZrOCl_2$ (3 mL) were added to a porcelain boat, which was then placed in a vacuum drying oven and dried for 4 h. The same porcelain boat was placed in the tube furnace and treated at 500 °C for 4 h. As a result, the ZrO_2/CB/coal-tar-pitch-SAC was successfully fabricated (Figure 1).

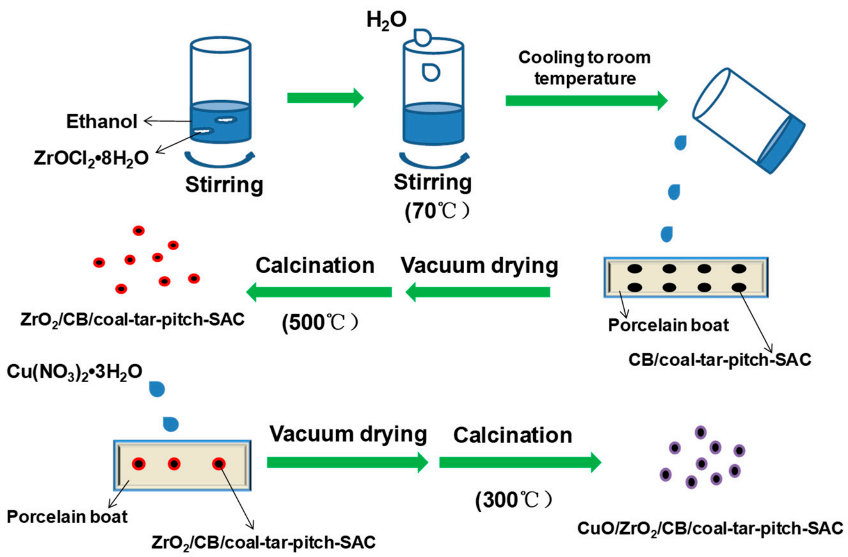

Figure 1. Images of fabrication process of CuO/ZrO_2/CB/coal-tar-pitch-SAC materials.

2.4. Preparation of CuO/ZrO_2/CB/Coal-Tar-Pitch-SAC

The ZrO_2/CB/coal-tar-pitch-SAC (1.3 g) was placed in three porcelain boats, and 0.5 M $Cu(NO_3)_2 \cdot 3H_2O$ solutions (0.75, 3.77 and 7.54 mL) were each dropped in these three porcelain boats. After these porcelain boats had been placed in the vacuum drying oven and dried for 4 h, they were placed in a tube furnace and treated at 300 °C for 2 h. According to the weight ratios (CuO:ZrO_2:CB/coal-tar-pitch-SAC = 0.03:0.3:1, 0.15:0.3:1 and 0.3:0.3:1), the prepared CuO/ZrO_2/CB/coal-tar-pitch-SAC materials were named as 0.03-CuO/ZrO_2/CB/coal-tar-pitch-SAC, 0.15-CuO/ZrO_2/CB/coal-tar-pitch-SAC and 0.3-CuO/ZrO_2/CB/coal-tar-pitch-SAC.

2.5. Sterilizing Tests of CuO/ZrO_2/CB/Coal-Tar-Pitch-SAC

The sterilization evaluations were performed using the spread plate method [27]. All experiment appliances were firstly used to perform sterilization treatments. The xenon lamp as a visible light source was used to conduct the sterilization of CuO/ZrO_2/CB/coal-tar-pitch-SAC materials. The CuO/ZrO_2/CB/coal-tar-pitch-SAC (0.1 g) was placed in a beaker (50 mL) containing koi fish feeding water (20 mL). Sterilization of CuO/ZrO_2/CB/coal-tar-pitch-SAC was performed for 1 h under irradiation of the xenon lamp. The sterilization efficiency was evaluated with the spread plate method.

3. Results and Discussion

The structures of CuO/ZrO_2/CB/coal-tar-pitch-SAC were primarily investigated by XRD measurements (Figure 2). In accordance with standards of CuO (ICOD 00-041-0254) and ZrO_2 (ICOD 00-049-1642), it was found that CuO, ZrO_2 and CuO/ZrO_2/CB/coal-tar-pitch-SAC materials were synthesized successfully. Additionally, it was observed that peak intensities of CuO remarkably increased with the amount of CuO.

The distributions of metal oxides on the surface were investigated by SEM measurements. Figure 3a shows that 0.03-CuO/ZrO_2/CB/coal-tar-pitch-SAC possessed an average diameter of around 200 µm. Figure 3b reveals that the agglomeration phenomenon of ZrO_2 coated on the surface of CB/coal-tar-pitch-SAC was scarcely noticeable. In contrast, the CuO was distinctly and uniformly covered on the surface of CB/coal-tar-pitch-SAC (Figure 3c).

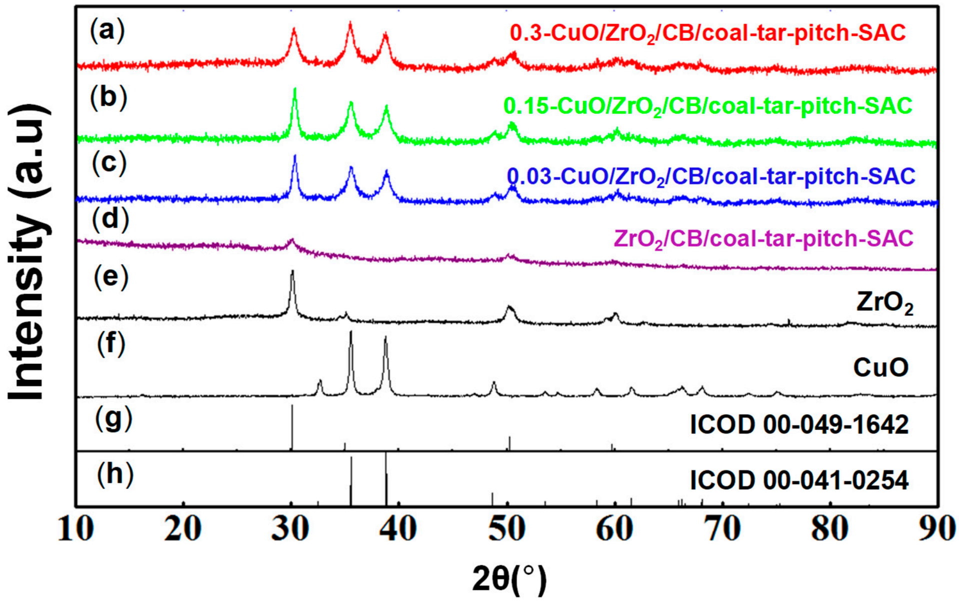

Figure 2. XRD results of CuO/ZrO_2/CB/coal-tar-pitch-SAC materials (**a**–**c**), ZrO_2/CB/coal-tar-pitch-SAC; (**d**), ZrO_2; (**e**), CuO; (**f**), standard of ICOD 00-049-1642 of ZrO_2; (**g**) and standard of ICOD 00-041-0254 of CuO (**h**).

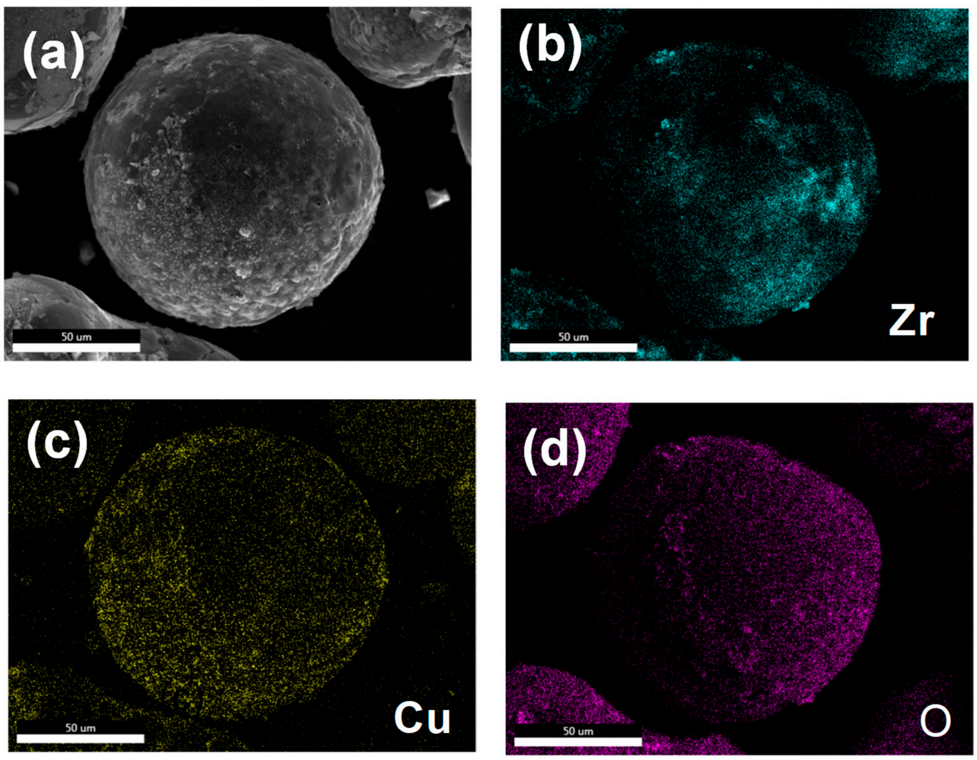

Figure 3. SEM (**a**) and SEM-EDS (**b**–**d**) images of 0.03-CuO/ZrO_2/CB/coal-tar-pitch-SAC material. EDS mapping of (**b**) Zr, (**c**) Cu and (**d**) O.

The BET method was used to investigate the pore structures and specific surface areas of CB/coal-tar-pitch-SAC, ZrO_2/CB/coal-tar-pitch-SAC and CuO/ZrO_2/CB/coal-tar-pitch-SAC materials (Figure 4). It was observed that CB/coal-tar-pitch-SAC manifested the largest specific surface area (1321.8 m^2/g) and total pore volume (0.52 cm^3/g) compared to ZrO_2/CB/coal-tar-pitch-SAC and CuO/ZrO_2/CB/coal-tar-pitch-SAC materials (Figure 3e, Table 1). With ZrO_2 and CuO covering the surface of CB/coal-tar-pitch-SAC, the specific surface area and total pore volume showed obviously diminished tendencies, attributed to the dispersal of ZrO_2 and CuO on the CuO/ZrO_2/CB/coal-tar-pitch-SAC materials (Figure 3a–d).

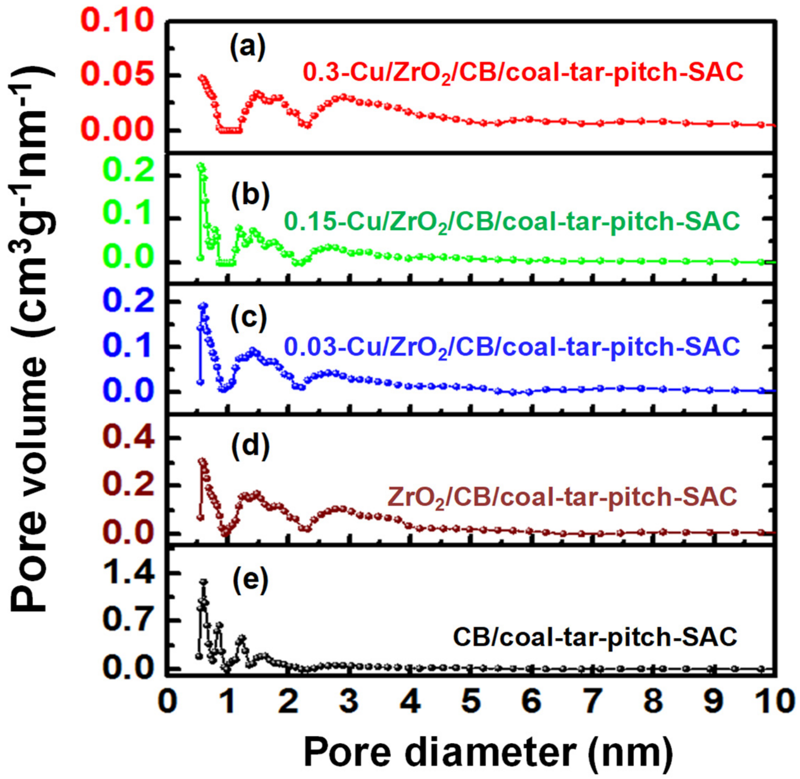

Figure 4. Pore size distribution curves of CB/coal-tar-pitch-SAC (**e**), ZrO_2/CB/coal-tar-pitch-SAC (**d**) and CuO/ZrO_2/CB/coal-tar-pitch-SAC materials (**a**–**c**).

Table 1. Characteristic parameters of structures and specific surface areas of CB/coal-tar-pitch-SAC, ZrO_2/CB/coal-tar-pitch-SAC and CuO/ZrO_2/CB/coal-tar-pitch-SAC materials. S_{BET} = total BET surface area; V_{total} = total pore volume.

Samples	S_{BET} ($m^2 \cdot g^{-1}$)	V_{total} ($cm^3 \cdot g^{-1}$)
CB/coal-tar-pitch-SAC	1321.8	0.52
ZrO_2/CB/coal-tar-pitch-SAC	631.6	0.49
0.03-CuO/ZrO_2/CB/coal-tar-pitch-SAC	330.8	0.24
0.15-CuO/ZrO_2/CB/coal-tar-pitch-SAC	210.6	0.19
0.3-CuO/ZrO_2/CB/coal-tar-pitch-SAC	131.9	0.17

The formation of a heterojunction among the ZrO_2 and CuO on the surface of CB/coal-tar-pitch-SAC was also verified by the XPS measurements. With increased CuO, the binding energy of $3d_{5/2}$ of ZrO_2 became stronger; however, the binding energy of $2p_{3/2}$ of CuO became slightly smaller (Figure 5). These conversions of binding energies strongly supported the authentic formation of the heterojunction among the ZrO_2 and CuO compounds on the surface of CB/coal-tar-pitch-SAC materials [27].

Furthermore, UV–Vis diffuse reflection spectroscopy (DRS) measurements were carried out to investigate the improvement of photosensitivity of CuO/ZrO_2/CB/coal-tar-pitch-SAC powders with a heterojunction among the ZrO_2 and CuO. As shown in Figure 6, it is naturally considered that the strong absorptive intensity around 270 nm was attributed to the ZrO_2 on the surface of ZrO_2/CB/coal-tar-pitch-SAC [28]. Nevertheless, the ZrO_2/CB/coal-tar-pitch-SAC materials showed weak photosensitivity at an irradiation range of 400 to 800 nm. On the contrary, the CuO/ZrO_2/CB/coal-tar-pitch-SAC materials displayed relatively stronger absorptive intensity at the irradiation range of 400 to 800 nm, indicating that constructing the heterojunctions among the ZrO_2 and CuO compounds on the surface of CuO/ZrO_2/CB/coal-tar-pitch-SAC materials is an efficacious method to enhance photosensitive ability under visible light.

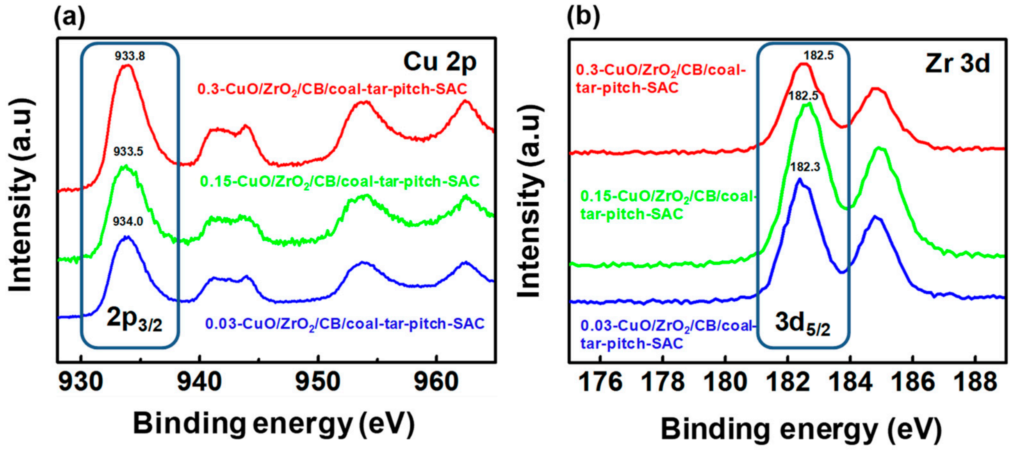

Figure 5. XPS results of Cu $2p_{3/2}$ (**a**) and Zr $3d_{5/2}$ (**b**) in CuO/ZrO_2/CB/coal-tar-pitch-SAC composite materials.

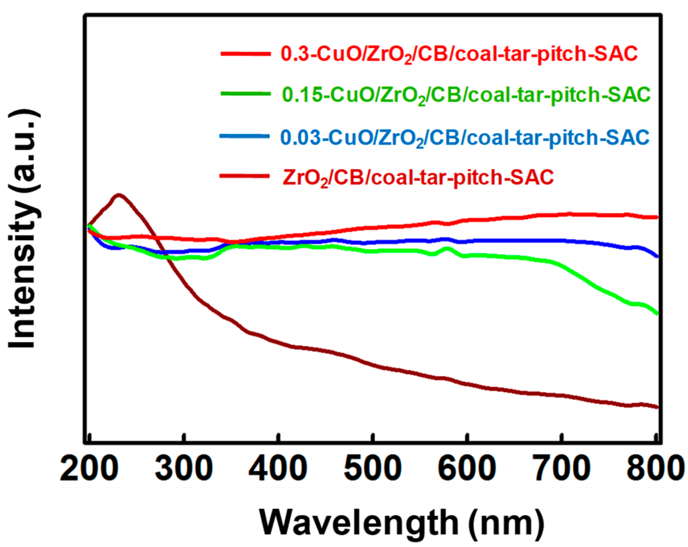

Figure 6. UV–Vis diffuse reflection spectroscopy (DRS) results of ZrO_2/CB/coal-tar-pitch-SAC and CuO/ZrO_2/CB/coal-tar-pitch-SAC powders.

Interestingly, it is obvious that 0.03-CuO/ZrO_2/CB/coal-tar-pitch-SAC showed stronger photosensitivity than 0.15-CuO/ZrO_2/CB/coal-tar-pitch-SAC at irradiation wavelengths of 400–800 nm (Figure 6). The carrier principle of transfer was used to fully explore the aforementioned phenomenon. The report by Lou et al. may explain these findings [29]. Namely, when the CuO/ZrO_2/CB/coal-tar-pitch-SAC powders were irradiated by visible light, many produced carriers on the CuO were able to be moved onto the surface of ZrO_2 compounds. Generally, with increased CuO, the produced number of carriers should be increased remarkably. However, the problem of electron-hole recombination diminishes the number of produced carriers. Consequently, the photosensitivity of 0.03-CuO/ZrO_2/CB/coal-tar-pitch-SAC is stronger than that of 0.15-CuO/ZrO_2/CB/coal-tar-pitch-SAC.

On the other hand, many CuO compounds on the surface of 0.3-CuO/ZrO_2/CB/coal-tar-pitch-SAC naturally enhanced the photosensitive ability because CuO possesses a narrow valance band. According to the Kubelka–Munk energy curve, the band gap energy (Eg) of different materials is described in Figure 7. It is observed that 0.3-CuO/ZrO_2/CB/coal-tar-pitch-SAC possessed smaller Eg than other materials, which was attributed to 0.3-CuO/ZrO_2/CB/coal-tar-pitch-SAC possessing more CuO than that in other materials [19].

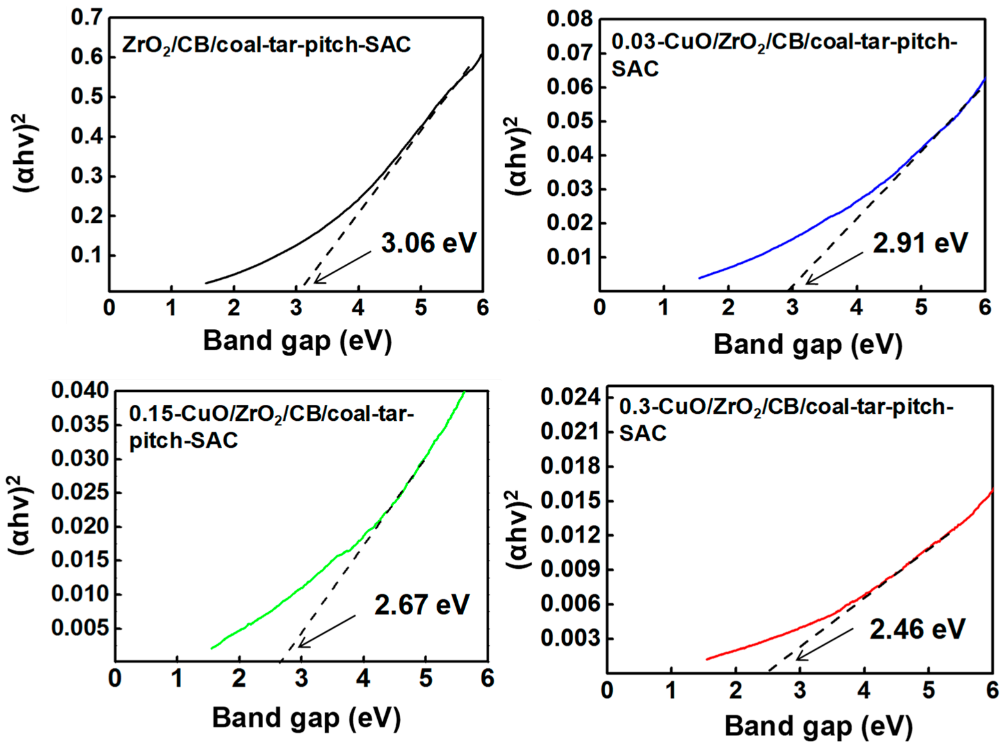

Figure 7. Plot of transformed Kubelka–Munk function versus the band gap (eV) of different samples.

The sterilization effects of CuO/ZrO_2/CB/coal-tar-pitch-SAC materials are illustrated in Figure 8. As shown in Figure 8b, the ZrO_2/CB/coal-tar-pitch-SAC did not show an obvious sterilization effect in visible light. On the other hand, the CuO/ZrO_2/CB/coal-tar-pitch-SAC materials showed obvious sterilization capacity in the same light conditions (Figure 8c–e). The 0.03-CuO/ZrO_2/CB/coal-tar-pitch-SAC exhibited an especially strong sterilization effect (Figure 8c).

In addition, the spread plate method was used to accurately evaluate the sterilization efficiency. As a result, it was also observed that the 0.03-CuO/ZrO_2/CB/coal-tar-pitch-SAC showed a significantly improved sterilization efficiency (94%) compared to 0.15-CuO/ZrO_2/CB/coal-tar-pitch-SAC (76%) and 0.3-CuO/ZrO_2/CB/coal-tar-pitch-SAC (84%). Considering the fact that 0.03-CuO/ZrO_2/CB/coal-tar-pitch-SAC possesses a larger specific surface area than other materials, the cooperative effects of formation of heterojunctions and large specific surface areas are the pivotal factors in improving the visible light sterilization capacity of CuO/ZrO_2/CB/coal-tar-pitch-SAC materials (Figure 9).

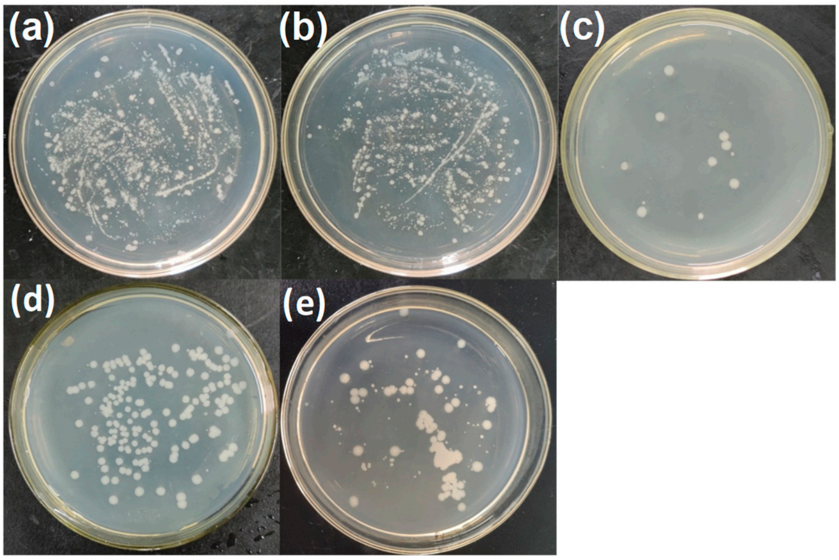

Figure 8. Evaluation of bactericidal effects. (**a**) Culturing result of the koi fish feeding water; (**b**) bactericidal effect of ZrO_2/CB/coal-tar-pitch-SAC in irradiation of visible light; (**c**) bactericidal effect of 0.03-CuO/ZrO_2/CB/coal-tar-pitch-SAC in visible light; (**d**) result of the water treated with the 0.15-CuO/ZrO_2/CB/coal-tar-pitch-SAC; (**e**) result of the water treated with the 0.3-CuO/ZrO_2/CB/coal-tar-pitch-SAC in visible light.

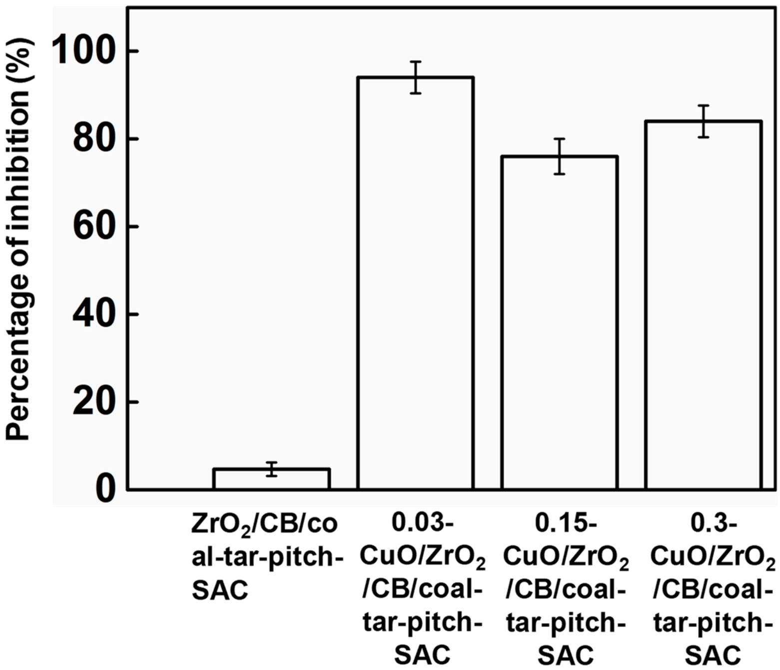

Figure 9. The sterilization effects of ZrO_2/CB/coal-tar-pitch-SAC and CuO/ZrO_2/CB/coal-tar-pitch-SAC materials.

4. Conclusions

CuO/ZrO_2/CB/coal-tar-pitch-SAC photocatalysts were successfully prepared by coating ZrO_2 and CuO on the surface of CB/coal-tar-pitch-SAC. It was found that the sterilization capacity of CuO/ZrO_2/CB/coal-tar-pitch-SAC was remarkably improved compared with the ZrO_2/CB/coal-tar-pitch-SAC. In particular, 0.03-CuO/ZrO_2/CB/coal-tar-pitch-SAC exhibits excellent sterilization efficiency at 94%, which is higher than other materials. The formation of a heterojunction among the CuO and ZrO_2 compounds facilitates the movement of carriers, which leads to CuO/ZrO_2/CB/coal-tar-pitch-SAC possessing the improved photosensitivity in visible light. Furthermore, the cooperative effects of formation of heterojunctions and large specific surface areas are the important factors in improving the visible light sterilization capacity of CuO/ZrO_2/CB/coal-tar-pitch-SAC materials. Our studies are able to provide a reference for fabrication of photocatalysts with visible light sterilization characteristics by constructing the heterojunction among the metal oxides on the surface of SAC materials. To realize the actual application of CuO/ZrO_2/CB/coal-tar-pitch-SAC, scale-up experiments of sterilization of aquaculture water will be performed in future.

Author Contributions: Conceptualization, Z.X. and W.Z.; methodology, K.W. and G.X.; validation, K.W., G.X. and B.H.; formal analysis, Z.X., L.L. and W.Z.; investigation, Z.X. and B.H.; resources, H.G. and B.A.; data curation, Z.X. and K.W.; writing—original draft preparation, Z.X.; writing—review and editing, W.Z.; supervision, D.J. and M.C.; project administration, B.A. All authors have read and agreed to the published version of the manuscript.

Funding: We are grateful for the support of the University of Science and Technology Liaoning (601009816-39 and 2017RC03). This work obtained support from the Liaoning Province Education Department of China (Grant No. 601009887-16). This work is partly supported by the project of the National Natural Science Foundation of China (Grant No. 51672117 and 51672118). This study is supported by the Postdoctoral Foundation Project of Shenzhen Polytechnic (6020330007K).

Institutional Review Board Statement: Not applicable.

Informed Consent Statement: Not applicable.

Data Availability Statement: Not applicable.

Conflicts of Interest: The authors declare no conflict of interest.

References

1. Jia, Q.; Song, Q.; Li, P.; Huang, W. Rejuvenated photodynamic therapy for bacterial infections. *Adv. Healthc. Mater.* **2019**, *8*, 1900608. [CrossRef] [PubMed]
2. Jia, R.; Tian, W.; Bai, H.; Zhang, J.; Wang, S.; Zhang, J. Sunlightdriven wearable and robust antibacterial coatings with water-soluble cellulose-based photosensitizers. *Adv. Healthc. Mater.* **2019**, *8*, 1801591. [CrossRef] [PubMed]
3. Qi, K.; Cheng, B.; Yu, J.; Ho, W. Review on the improvement of the photocatalytic and antibacterial activities of ZnO. *J. Alloys Compd.* **2017**, *727*, 792–820. [CrossRef]
4. Lee, M.M.S.; Xu, W.; Zheng, L.; Yu, B.; Leung, A.C.S.; Kwok, R.T.K.; Lam, J.W.Y.; Xu, F.J.; Wang, D.; Tang, B.Z. Ultrafast discrimination of Gram-positive bacteria and highly efficient photodynamic antibacterial therapy using near-infrared photosensitizer with aggregation-induced emission characteristics. *Biomaterials* **2020**, *230*, 119582. [CrossRef] [PubMed]
5. Ahmed, B.; Ojha, A.K.; Singh, A.; Hirsch, F.; Fischer, I.; Patrice, D.; Materny, A. Well-controlled in-situ growth of 2D WO_3 rectangular sheets on reduced graphene oxide with strong photocatalytic and antibacterial properties. *J. Hazard. Mater.* **2018**, *347*, 266–278. [CrossRef] [PubMed]
6. Kim, B.C.; Jeong, E.; Kim, E.; Hong, S.W. Bio-organic-inorganic hybrid photocatalyst, TiO_2 and glucose oxidase composite for enhancing antibacterial performance in aqueous environments. *Appl. Catal.* **2019**, *242*, 194–201. [CrossRef]
7. Fujishima, A.; Honda, K. Electrochemical photolysis of water at a semiconductor electrode. *Nature* **1972**, *238*, 37–38. [CrossRef]
8. Wang, Y.; Zhao, D. On the controllable soft-templating approach to mesoporous silicates. *Chem. Rev.* **2007**, *107*, 2821–2831.
9. Yamamoto, O.; Sawai, J.; Sasamoto, T. Activated carbon sphere with antibacterial characteristics. *Mater. Trans.* **2005**, *43*, 1069–1073. [CrossRef]
10. Shen, L.Z.; Xu, G.Y.; Han, B.B.; Kato, S.K.; Dai, Y.Y.; Ge, H.; Wang, K.; Sun, F.; Zhou, W.M. Study on fabrication and sterilization characteristics of novel composite spherical activated carbon (TiO_2/CB/SAC). *J. Chem. Eng. Jpn.* **2020**, *53*, 526–532. [CrossRef]
11. Hirvonen, A.; Nowak, R.; Yamamoto, Y.; Sekino, T.; Niihara, K. Fabrication, structure, mechanical and thermal properties of zirconia-based ceramic nanocomposites. *J. Eur. Ceram. Soc.* **2006**, *26*, 1497–1505. [CrossRef]
12. Chandra, N.; Singh, D.K.; Sharma, M.; Upadhyay, R.K.; Amritphale, S.S.; Sanghi, S.K. Synthesis and characterization of nano-sized zirconia powder synthesized by single emulsion-assisted direct precipitation. *J. Colloid. Interf. Sci.* **2010**, *342*, 327–332. [CrossRef] [PubMed]
13. Kaviyarasu, K.; Kotsedi, L.; Simo, A.; Fuku, X.; Mola, G.T.; Kennedy, J.; Maaza, M. Photocatalytic activity of ZrO_2 doped lead dioxide nanocomposites: Investigation of structural and optical microscopy of RhB organic dye. *Appl. Surf. Sci.* **2016**, *421*, 234–239. [CrossRef]
14. Qin, Y.M.; Ding, Z.Y.; Guo, W.W.; Guo, X.L.; Hou, C.; Jiang, B.P.; Liu, C.G.; Shen, X.C. A full solar light spectrum responsive B@ZrO_2–OV photocatalyst: A synergistic strategy for visible-to-NIR photon harvesting. *ACS Sustain. Chem. Eng.* **2020**, *8*, 13039–13047. [CrossRef]

15. Fechete, I.; Ye, W.; Védrine, J.C. The past, present and future of heterogeneous catalysis. *Catal. Today* **2012**, *189*, 2–27. [CrossRef]
16. Yu, S.; Liu, J.; Yan, Z.; Richard, D.W.; Yan, X.L. Effect of synthesis method on the nanostructure and solar-driven photocatalytic properties of TiO_2-CuS composites. *ACS Sustain. Chem. Eng.* **2017**, *5*, 1347–1357. [CrossRef]
17. Li, J.X.; Guan, R.Q.; Zhang, J.K.; Zhao, Z.; Zhai, H.J.; Sun, D.W.; Qi, Y.F. Preparation and photocatalytic performance of dumbbell Ag_2CO_3-ZnO heterojunctions. *ACS Omega* **2020**, *5*, 570–577. [CrossRef] [PubMed]
18. Li, J.Q.; Cui, M.M.; Guo, Z.; Liu, Z.X.; Zhu, Z.F. Synthesis of dumbbell-like CuO–$BiVO_4$ heterogeneous nanostructures with enhanced visible-light photocatalytic activity. *Mater. Lett.* **2014**, *130*, 36–39. [CrossRef]
19. Zhang, J.; Li, L.; Xiao, Z.Y.; Liu, D.; Wang, S.; Zhang, J.J.; Hao, Y.T.; Zhang, W.Z. Hollow sphere TiO_2–ZrO_2 prepared by self-assembly with polystyrene colloidal template for both photocatalytic degradation and H_2 evolution from water splitting. *ACS Sustain. Chem. Eng.* **2016**, *4*, 2037–2046. [CrossRef]
20. Ayodeji, P.A.; Reyes-Lopéz, S.Y. ZrO_2-ZnO nanoparticles as antibacterial agents. *ACS Omega* **2019**, *4*, 19216–19224.
21. Kargar, A.; Jing, Y.; Kim, S.J.; Riley, C.T.; Pan, X.Q.; Wang, D. ZnO/CuOheterojunction branched nanowires for photoelectrochemical hydrogen generation. *ACS Nano* **2013**, *7*, 11112–11120. [CrossRef]
22. Zhu, L.; Li, H.; Liu, Z.; Xia, P.; Xie, Y.; Xiong, D. Synthesis of 0D/3D CuO/ZnOheterojunction with enhanced photocatalytic activity. *J. Phys. Chem. B.* **2018**, *122*, 9531–9539.
23. Raees, A.; Jamal, M.A.; Ahmed, I.; Silanpaa, M.; Algarni, T.S. Synthesis and characterization of CeO_2/CuOnanocomposites for photocatalytic degradation of methylene blue in visible light. *Coatings* **2021**, *11*, 305. [CrossRef]
24. Zhang, Z.L.; Yang, Z.; Yang, H. Theoretical and practical discussion of measurement accuracy for physisorption with micro- and mesoporous materials. *Chin. J. Catal.* **2013**, *34*, 1797–1810. [CrossRef]
25. Hu, S.X.; Hsieh, Y.L. Lignin derived activated carbon particulates as an electric supercapacitor: Carbonization and activatioon porous structures and microstructures. *RSC Adv.* **2017**, *7*, 30459–30468. [CrossRef]
26. Kupgan, G.; Liyana-Arachchi, T.P.; Colina, C.M. NLDFT Pore Size Distribution in Amorphous Microporous Materials. *Langmuir* **2017**, *33*, 11138–11145. [CrossRef]
27. Gong, J.; Zhao, Z.J.; Wang, Z.; Luo, R.; Wang, Y. Strong electronic oxidesupport interaction over In_2O_3/ZrO_2 for highly selective CO_2 hydrogenation to methanol. *J. Am. Chem. Soc.* **2020**, *142*, 19523–19531.
28. Nova, C.V.; Reis, K.A.; Pinheiro, A.L.; Dalmaschio, C.J.; Chiquito, A.J.; Teodoro, M.D.; Rodrigues, A.D. Synthesis, characterization, photocatalytic, and antimicrobial activity of ZrO_2 nanoparticles and Ag@ZrO_2nanocomposite prepared by the advanced oxidative process/hydrothermal route. *J. Sol. Gel. Sci. Technol.* **2021**, *98*, 113–126. [CrossRef]
29. Lou, X.; Shang, J.; Liang, W.; Feng, H.; Hao, W.; Wang, T.; Du, Y. Enhanced photocatalytic activity of $Bi_{24}O_{31}Br_{10}$: Constructing heterojunction with BiOI. *J. Mater. Sci. Technol.* **2017**, *33*, 281–284. [CrossRef]